Institute of Space Sciences
EXCELENCIA MARÍA DE MAEZTU

Universitat Autònoma de Barcelona

The 2022 reactivation of the magnetar SGR J1935+2154

A. Ibrahim

The X-ray mysteries of Neutron Stars and White Dwarfs

European Space Astronomy Centre (ESAC)

Madrid, Spain

May 21st, 2024

NASA's Goddard Space Flight Center/Chris Smith (USRA/GESTAR)

Content

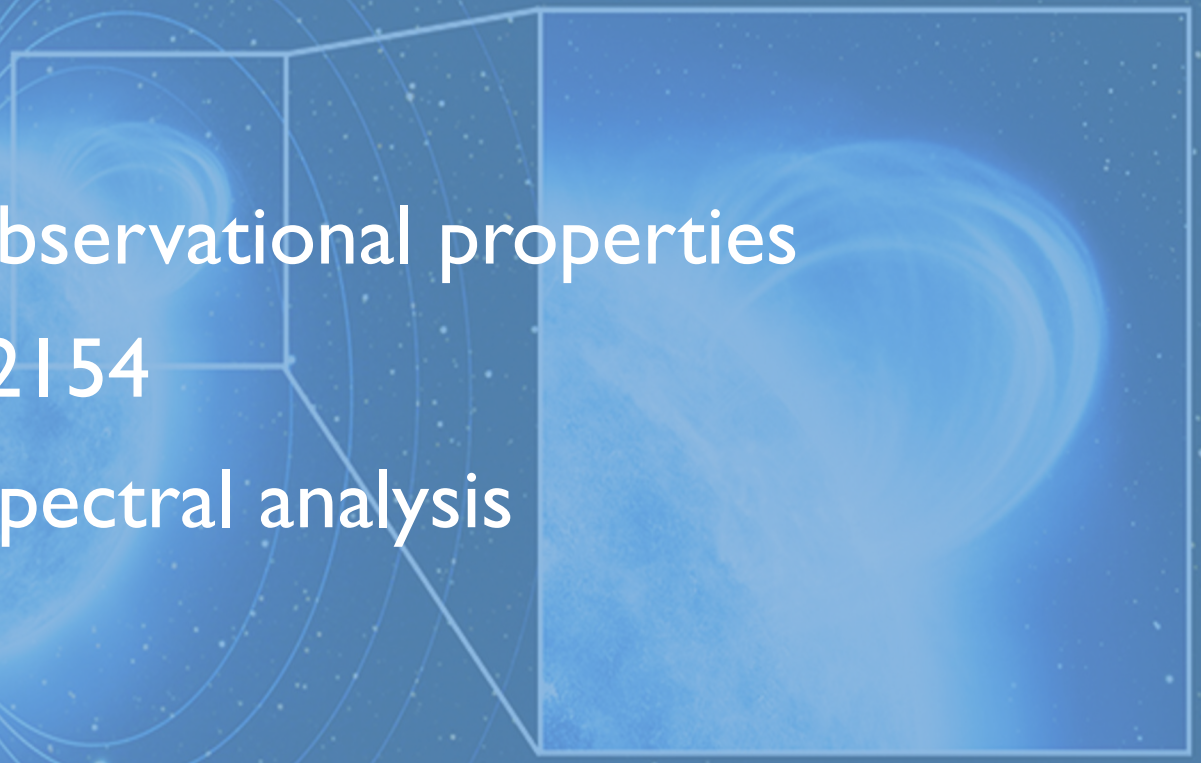

1. Magnetars: observational properties
2. SGR J1935+2154
3. Timing and spectral analysis
4. Conclusion

1.1. Magnetars in P&Pdot

- P ~ 0.3 – 12 s
- P_{dot} ~ 10^{-13} – 10^{-11} s s^{-1}
- B ~ 10^{14} --10^{15} G
- Persistent X-ray sources
  L_X ~ 10^{31} – 10^{36} erg s^{-1}
- Transient activity:
  - Bursts
  - Giant Flares
  - Outbursts

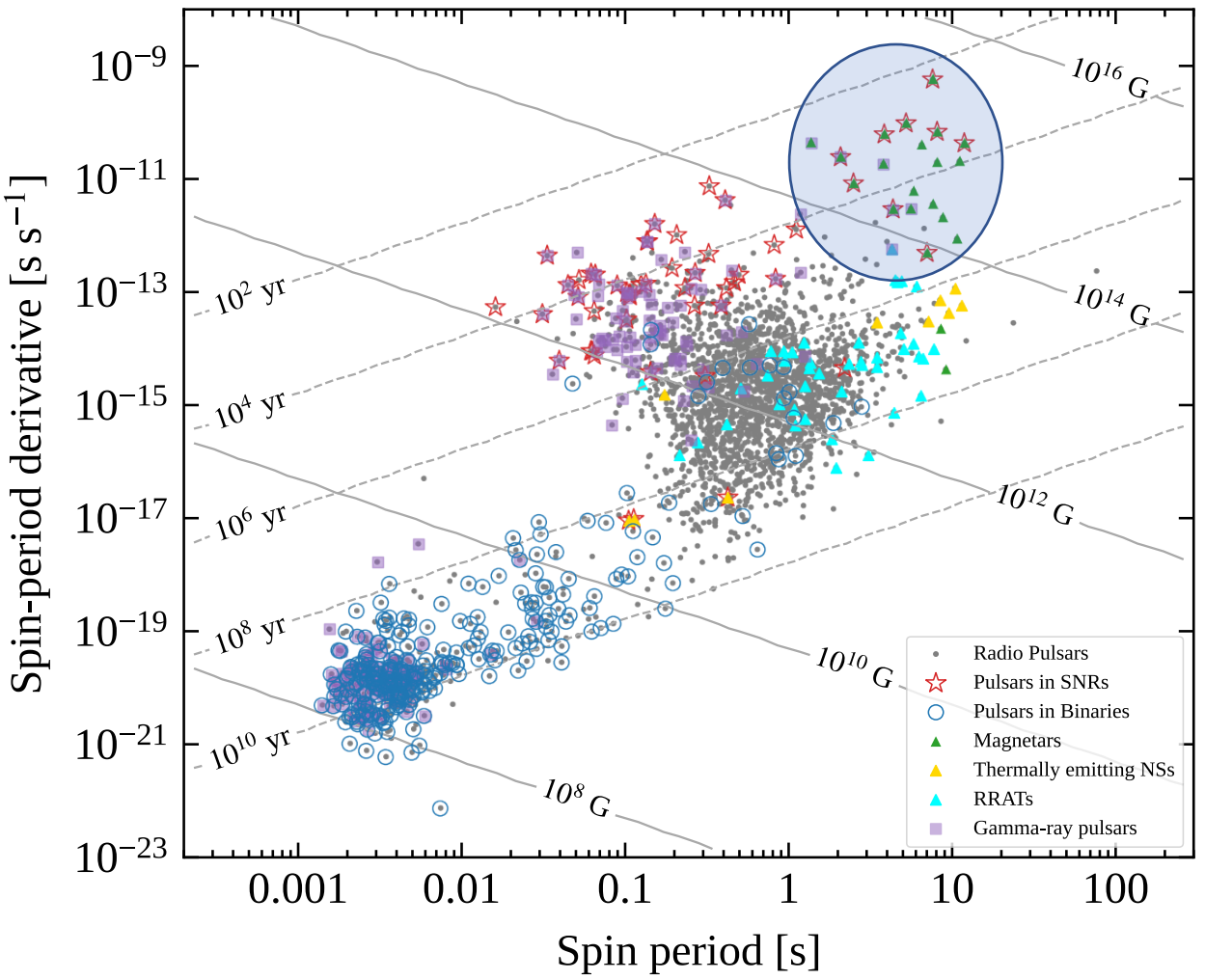

Duncan & Thompson et al. 1992; Kaspi & Beloborodov et al. 2017; Esposito et al. 2021. Fig: Ronchi PhD thesis. 2024

2. SGR J1935+2154

- 2014 July 5, Swift/BAT detected short bursts
- Follow-up observations with Swift, Chandra, and XMM-Newton
- P = 3.24 s
- $P_{dot} \sim 1.43 \times 10^{-11}$ s s^{-1}
- $B \sim 2.2 \times 10^{14}$ G

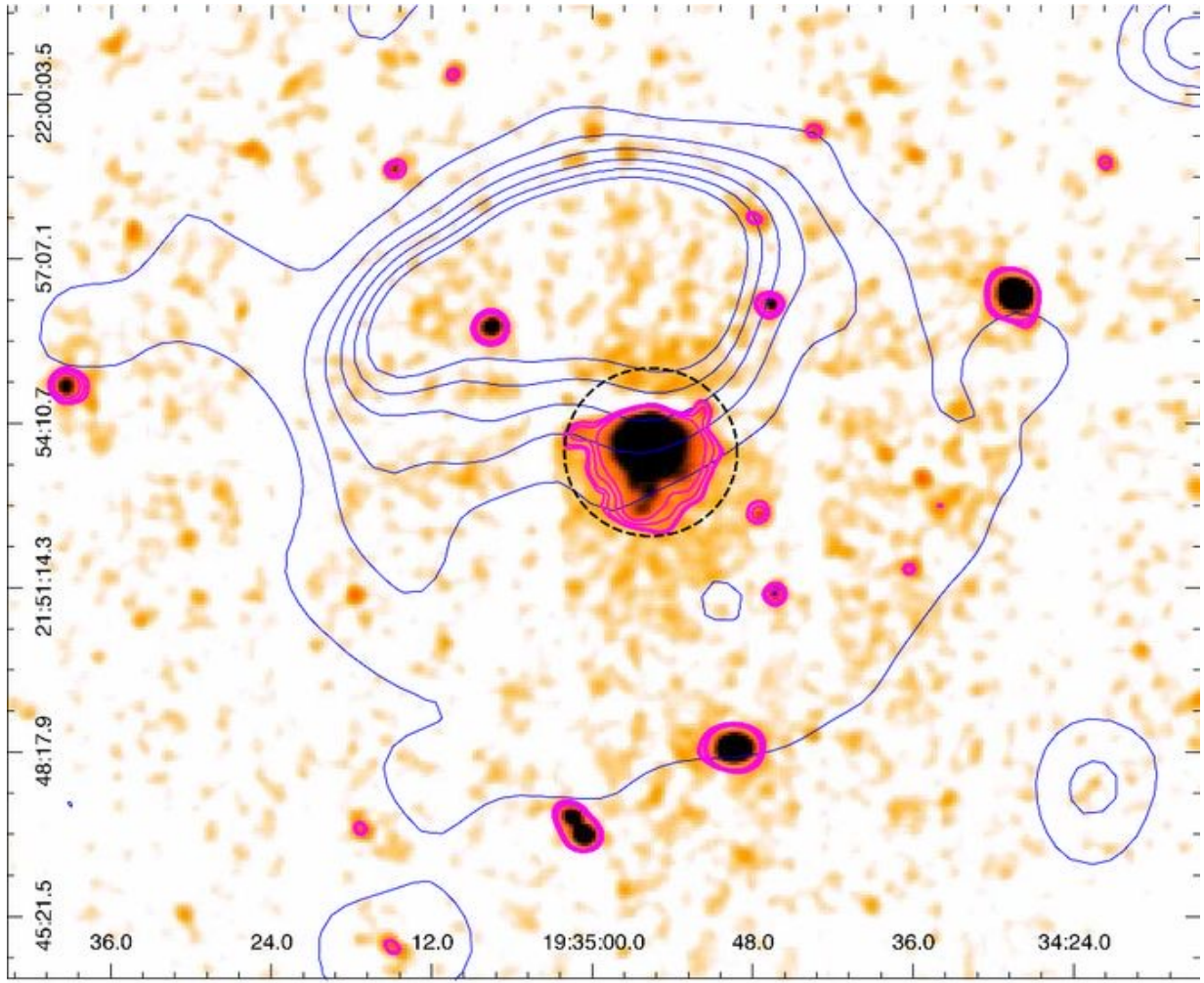

Stamatikos et al. 2014; Israel et al. 2016

2.1. SGR J1935+2154: Outbursts history

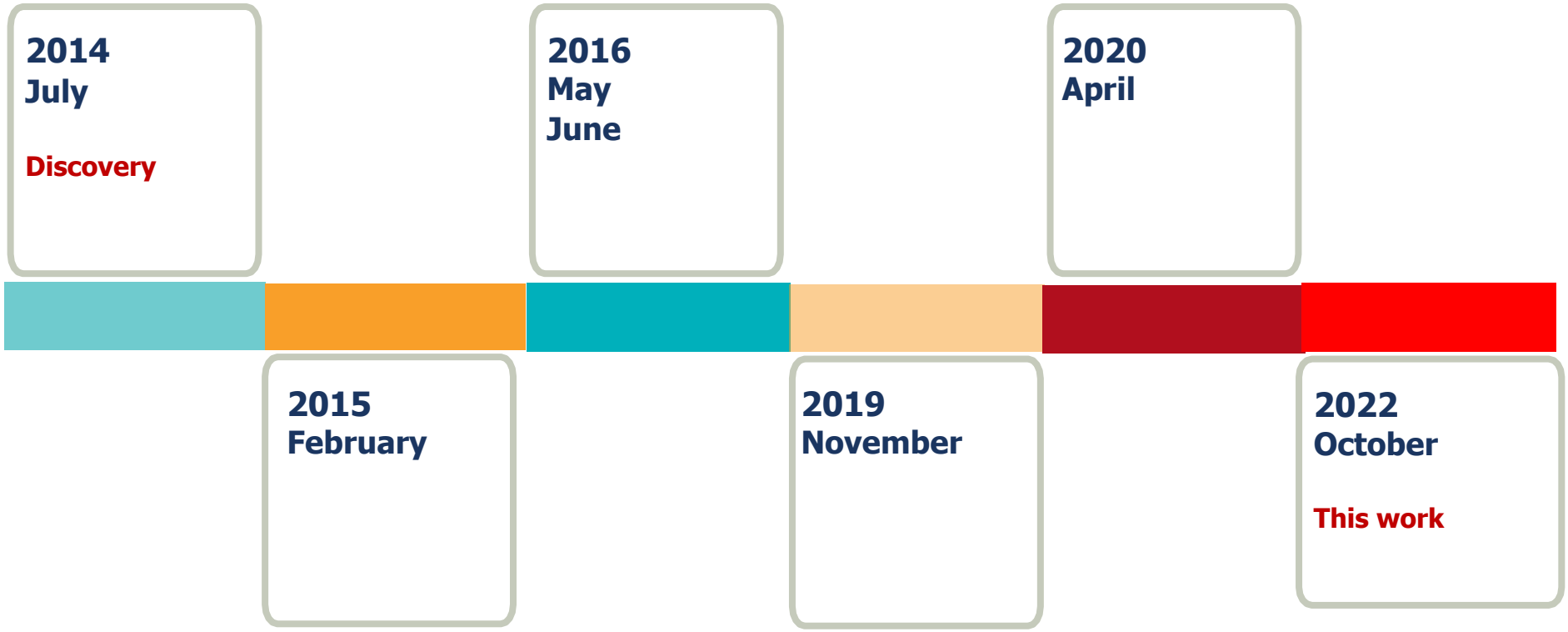

Israel et al. 2016; Younes et al. 2017,2020; Borghese et al. 2020, 2022; CHIME/FRB Collaboration et al. 2020, 2022; Ibrahim et al. 2022

2.1. SGR J1935+2154: X-ray & Radio bursts

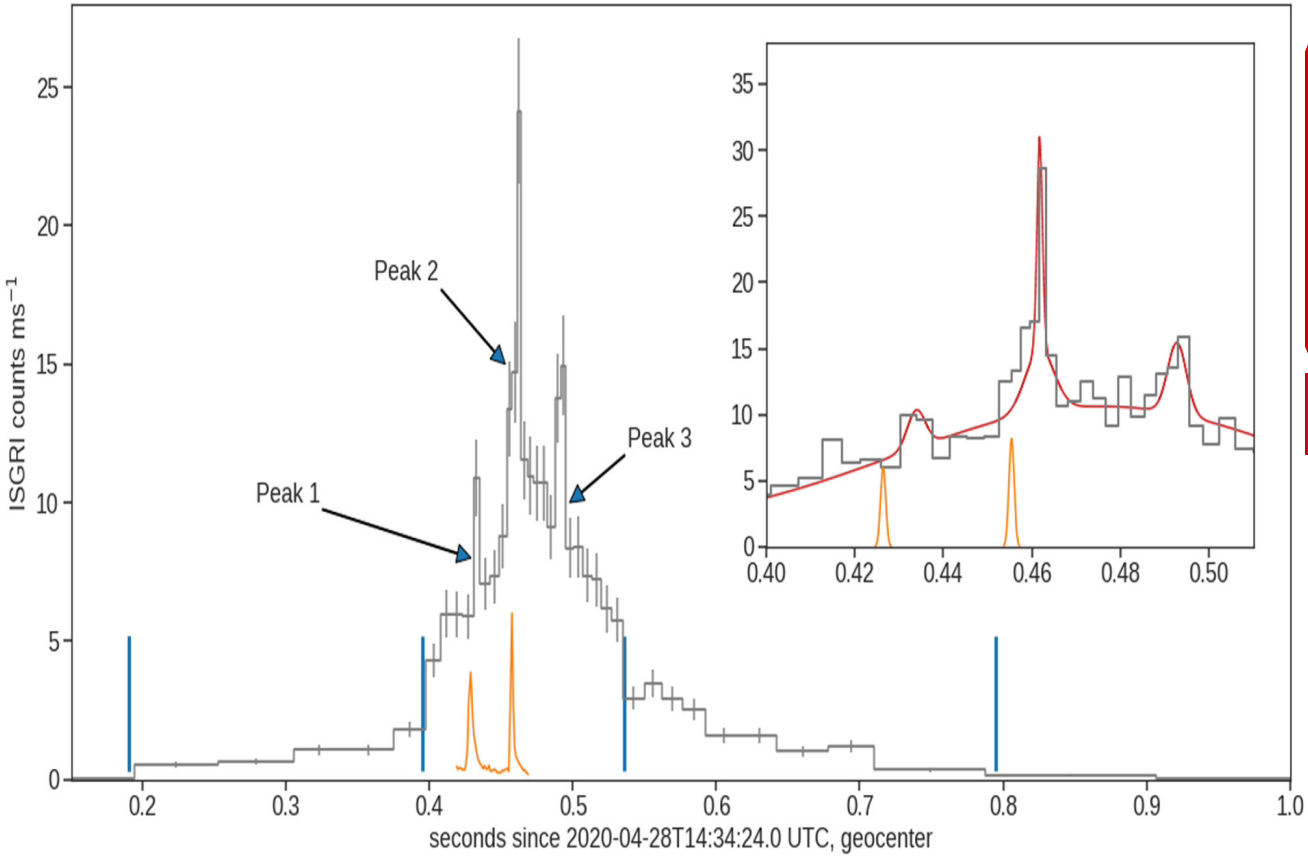

2020
April

Simultaneous hard X-ray bursts and double-peaked radio (FRB200428)

2022
October

This work

CHIME/FRB Collaboration et al. 2020b; Bochenek et al. 2020; Fig: Mereghetti et al 2020

2.1. SGR J1935+2154: X-ray & Radio bursts

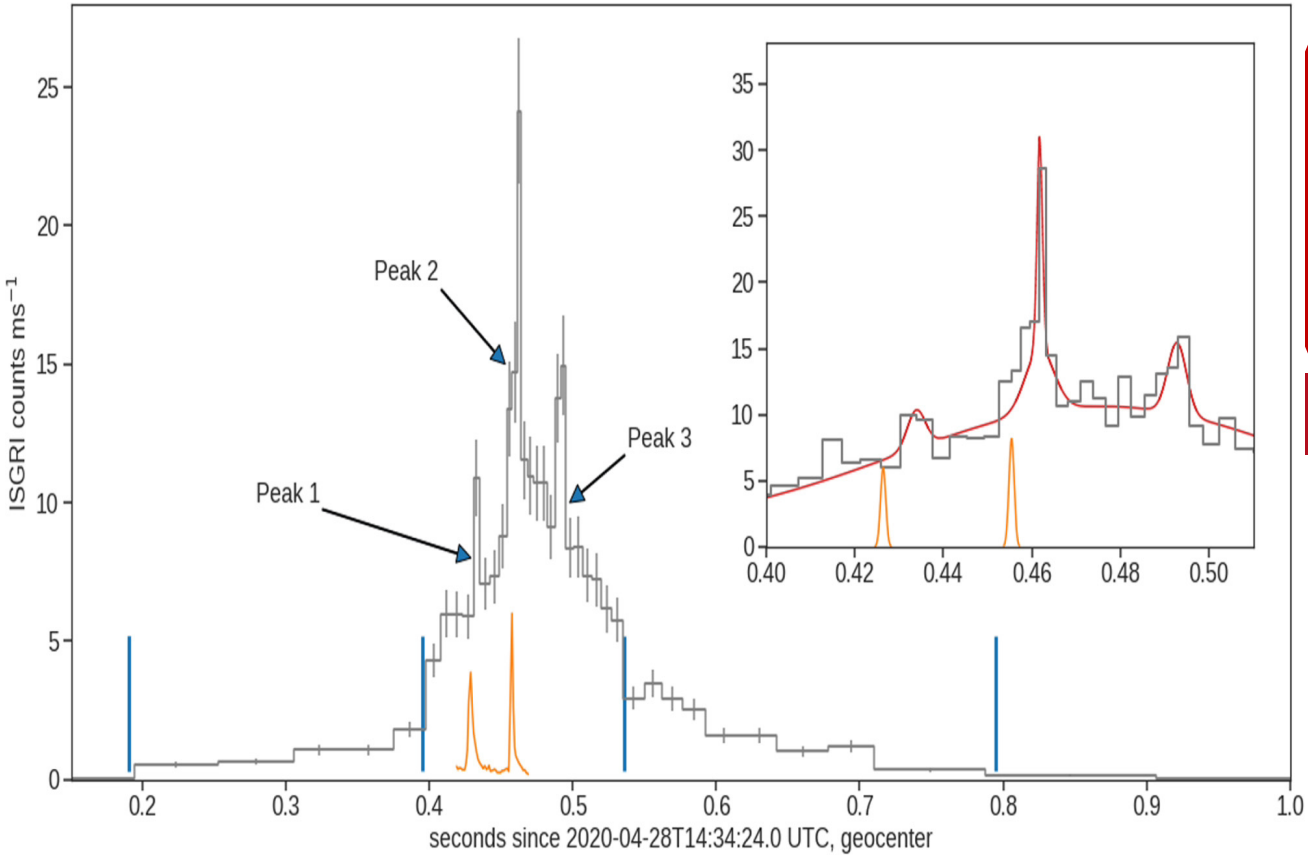

2020 April

Simultaneous hard X-ray bursts and double-peaked radio (FRB200428)

Magnetars as a model for FRBs

2022 October

This work

CHIME/FRB Collaboration et al. 2020b; Bochenek et al. 2020; Fig: Mereghetti et al 2020

2. Observations

XMM-Newton	NuSTAR	INTEGRAL
	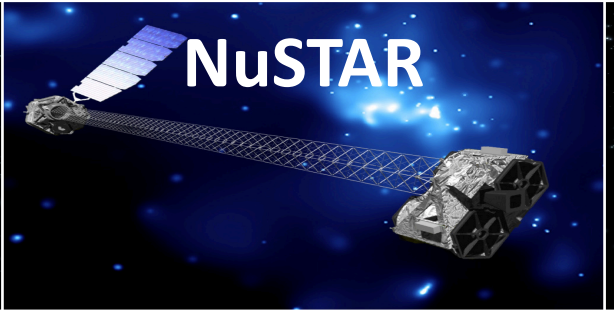	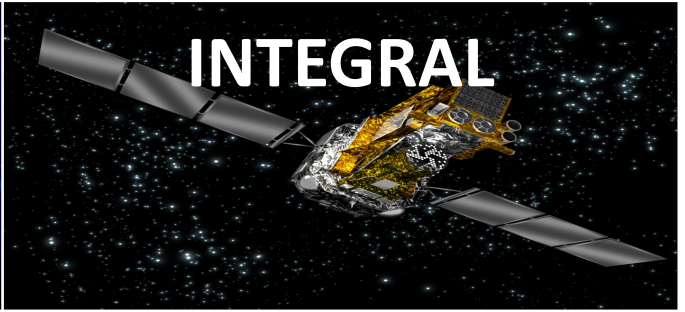
Two observations 2022 October 15-22	Two observations 2022 October 18-22	23 pointings 2022 October 15(18:51 UTC) - 16(0.4:47 UTC)
Total exposure ~ 90 ks	Total exposure ~ 100 ks	15-1000 keV

3.1. Timing analysis

- Phase-coherent timing (0.3--15keV)
- P ~ 3.25 s
- P_{dot} = 5.52 (5) X 10^{-11} s s^{-1}
- 3.8x larger than 2014 outburst ($1.43e^{-11}$)

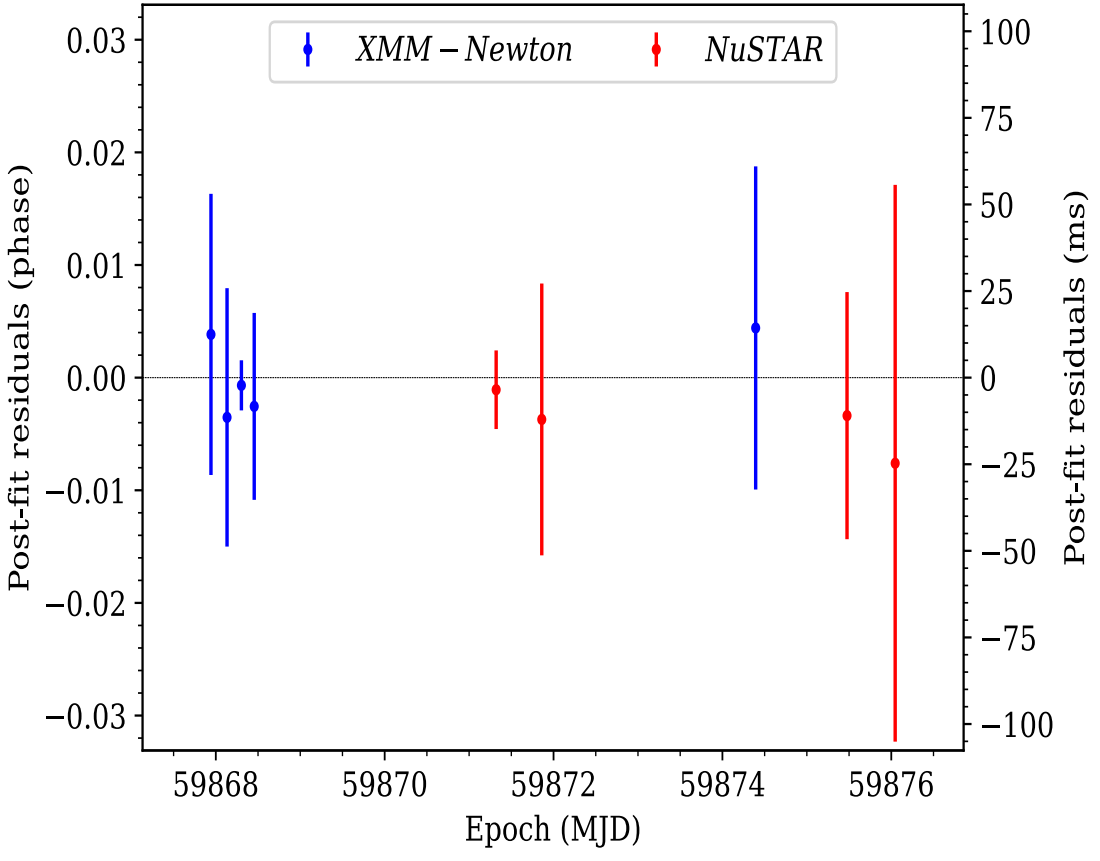

3.1. Timing analysis

- Phase-coherent timing (0.3--15keV)
- P ~ 3.25 s
- P_{dot} = 5.52 (5) X 10^{-11} s s^{-1}
- 3.8x larger than 2014 outburst ($1.43e^{-11}$)

  - Magnetospheric geometry
  - Relativistic winds of the magnetar

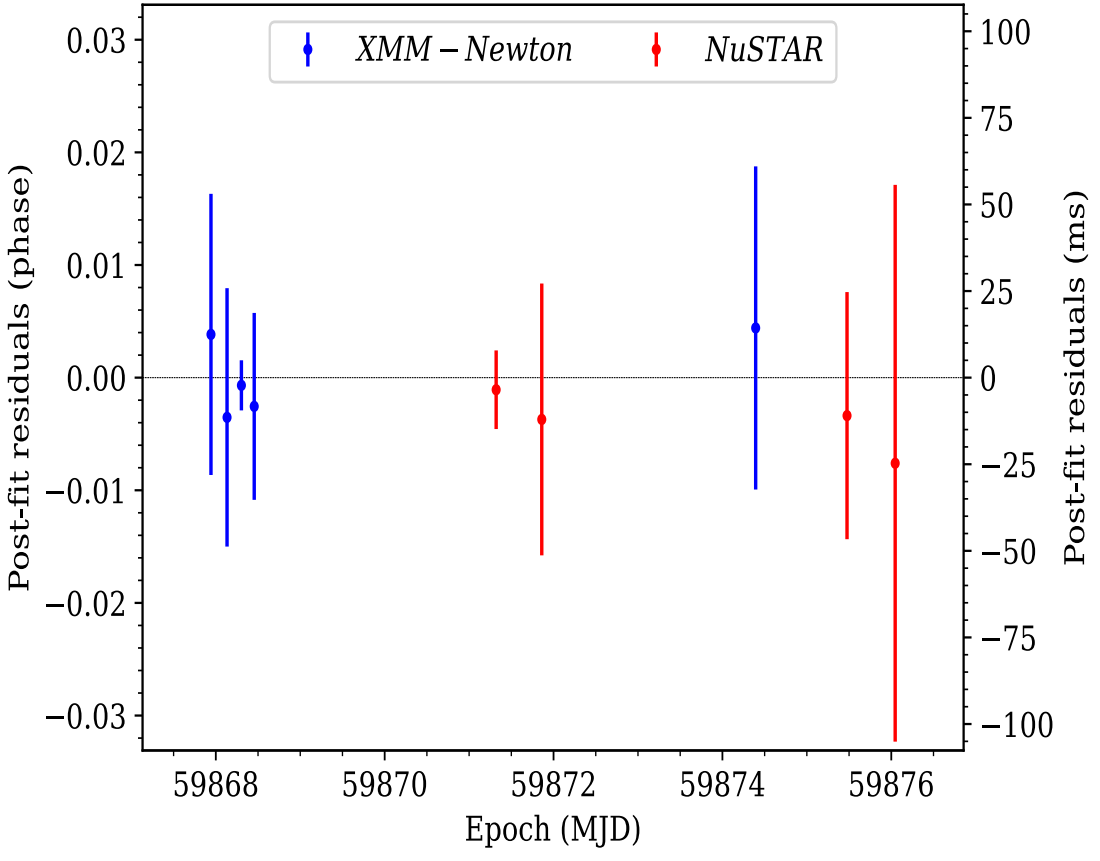

3.2. **Energy-resolved pulse profile**

- Cons + 2 sinusoidal function

(fundamental 1st harmonic components)

- Morphology evolution
- No specific trend in the PF

epoch1 (14-26) epoch2 (11-76)

$E_{25\text{-}79}$ (26 -76)

- Phase-resolved spectroscopy:

A phase shift: $soft_{(0.3-10)}$ /$hard_{(10-25)}$ (~$0.13_{P1Ep1,11}$ & $0.19_{PIIEp1,}0.22_{PIIEp2}$)

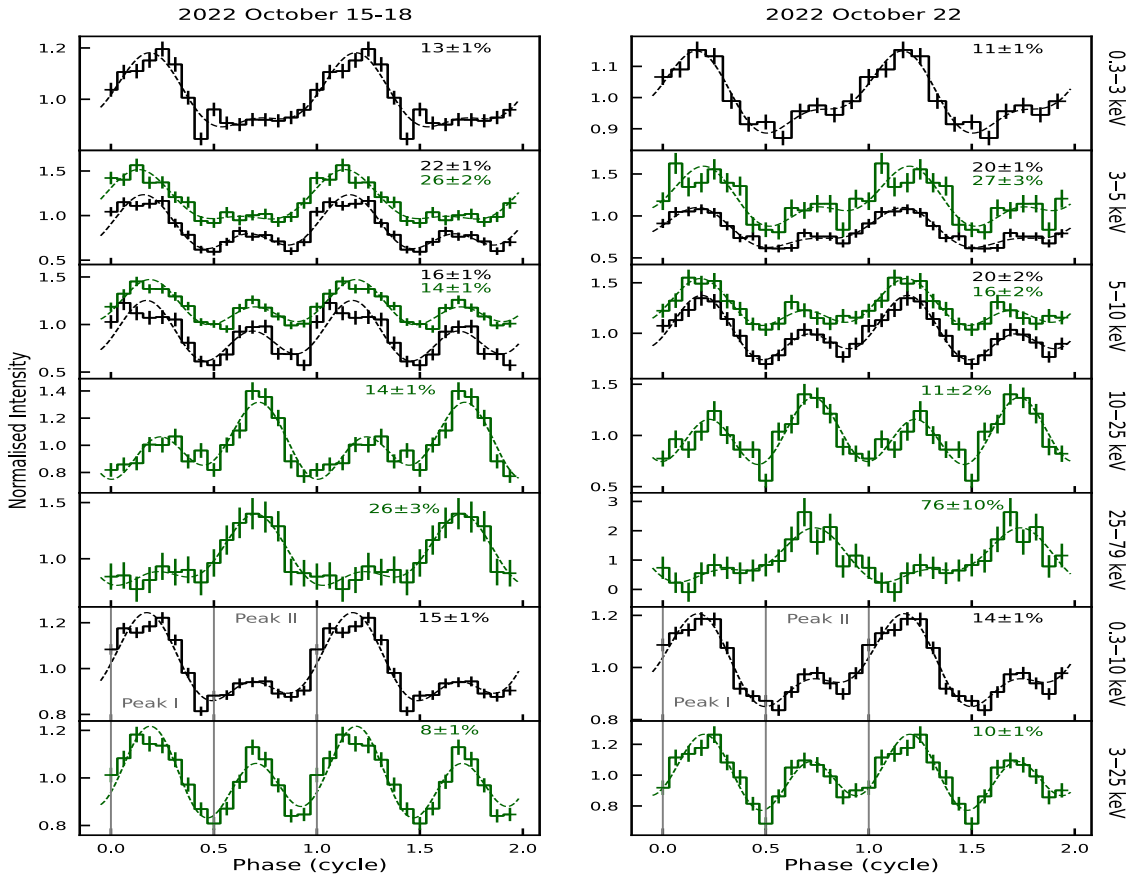

3.2. **Energy-resolved pulse profile**

- Cons + 2 sinusoidal function

(fundamental 1st harmonic components)

- Morphology evolution
- No specific trend in the PF

epoch1 (14-26) epoch2 (11-76)

$E_{25\text{-}79}$ (26 -76)

- Phase-resolved spectroscopy:

A phase shift: $soft_{(0.3-10)}$ /$hard_{(10-25)}$ (~$0.13_{P1Ep1,11}$ & $0.19_{PllEp1,}0.22_{PllEp2}$)

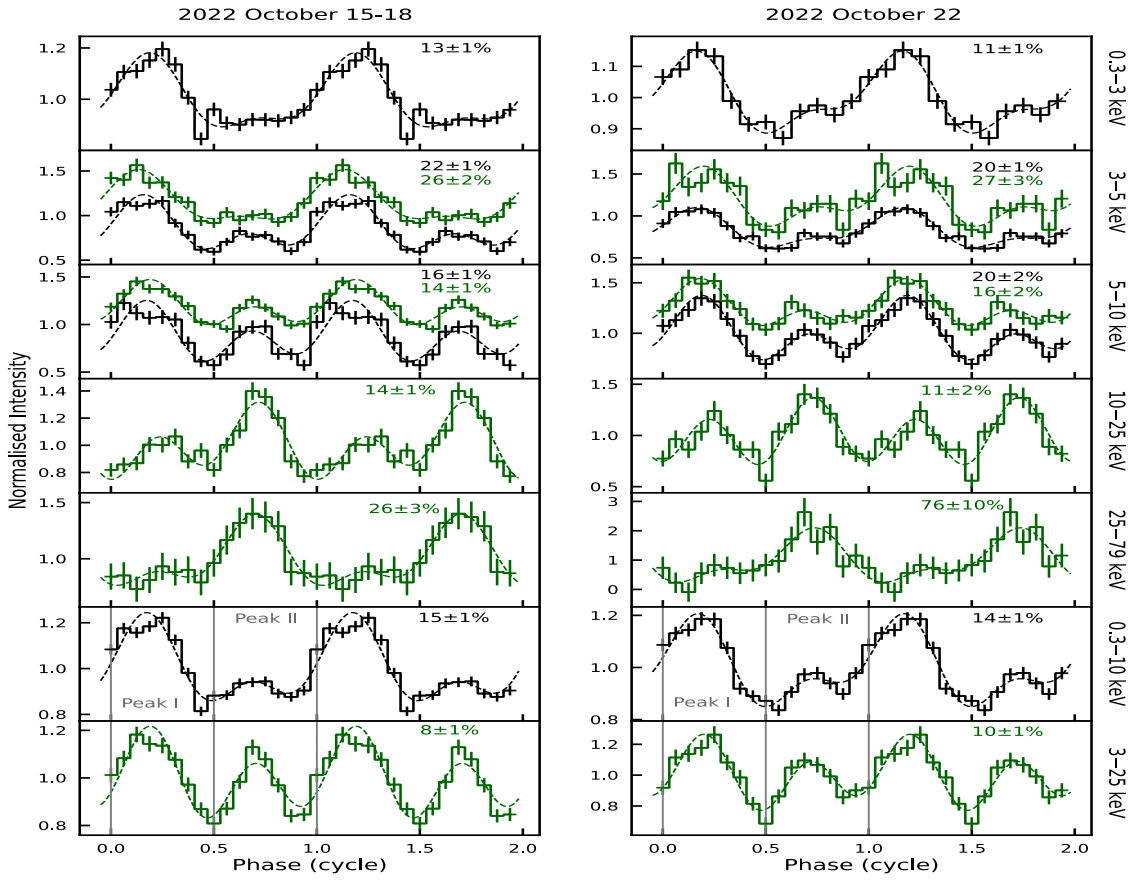

3.2. **Energy-resolved pulse profile**

- Cons + 2 sinusoidal function (fundamental 1st harmonic components)
- Morphology evolution

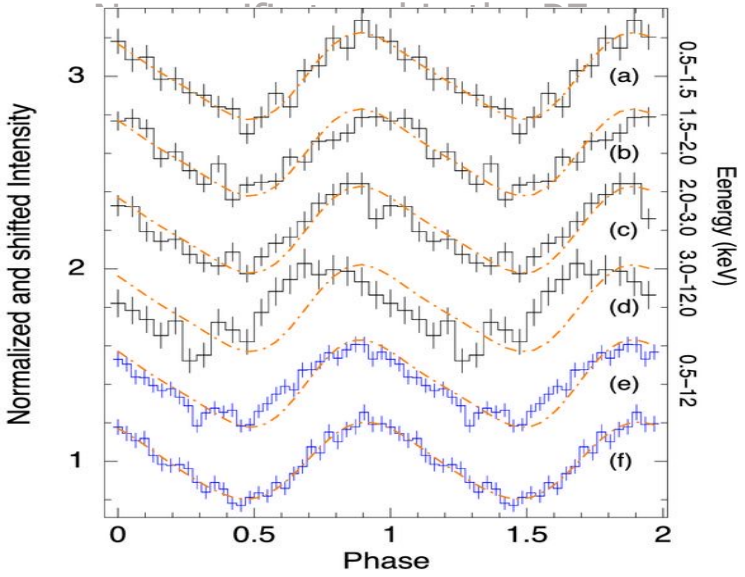

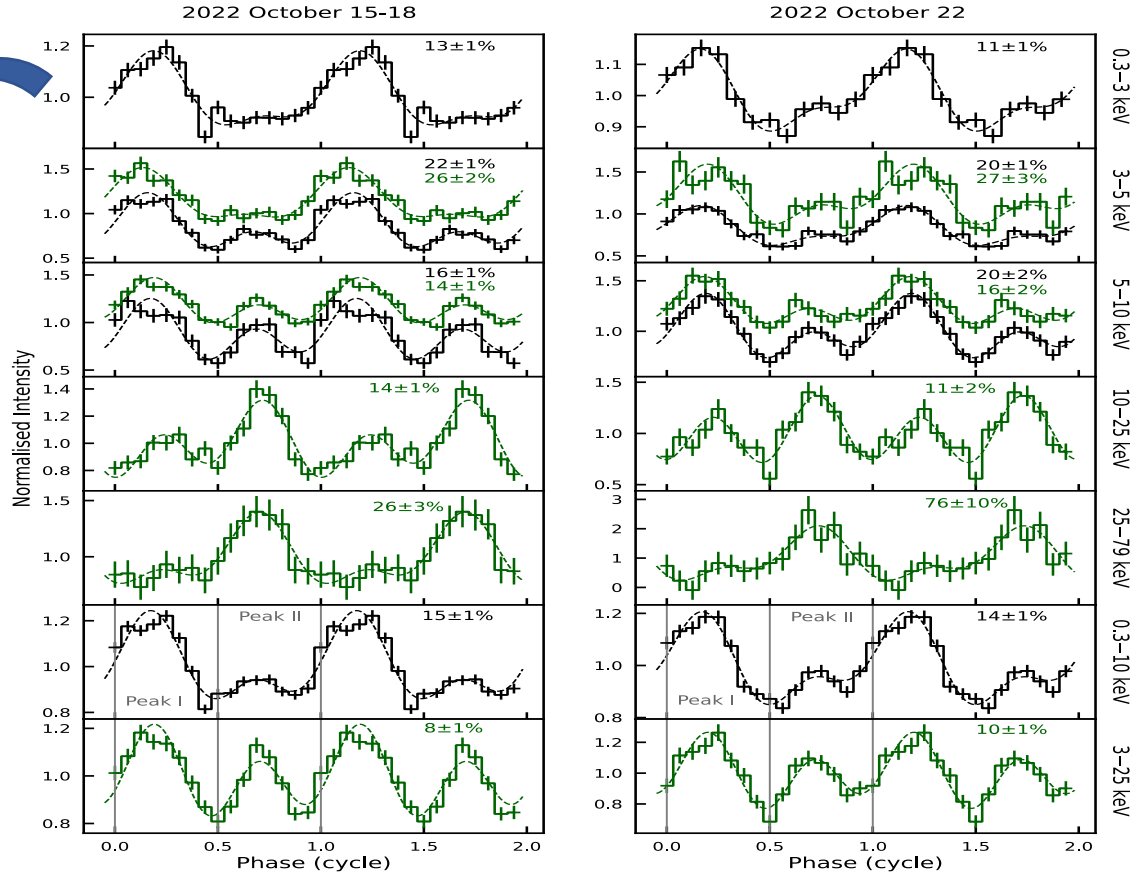

Israel et al. 2016

3.2. **Energy-resolved pulse profile**

- Cons + 2 sinusoidal function (fundamental 1st harmonic components)
- Morphology evolution

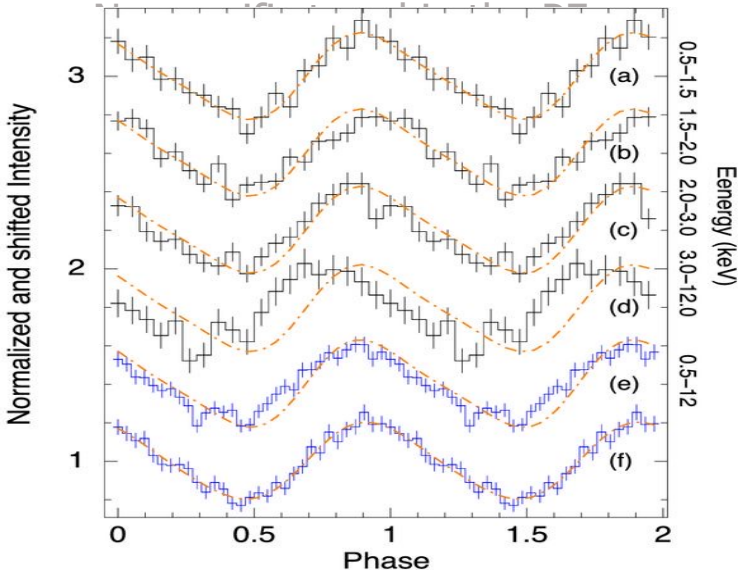

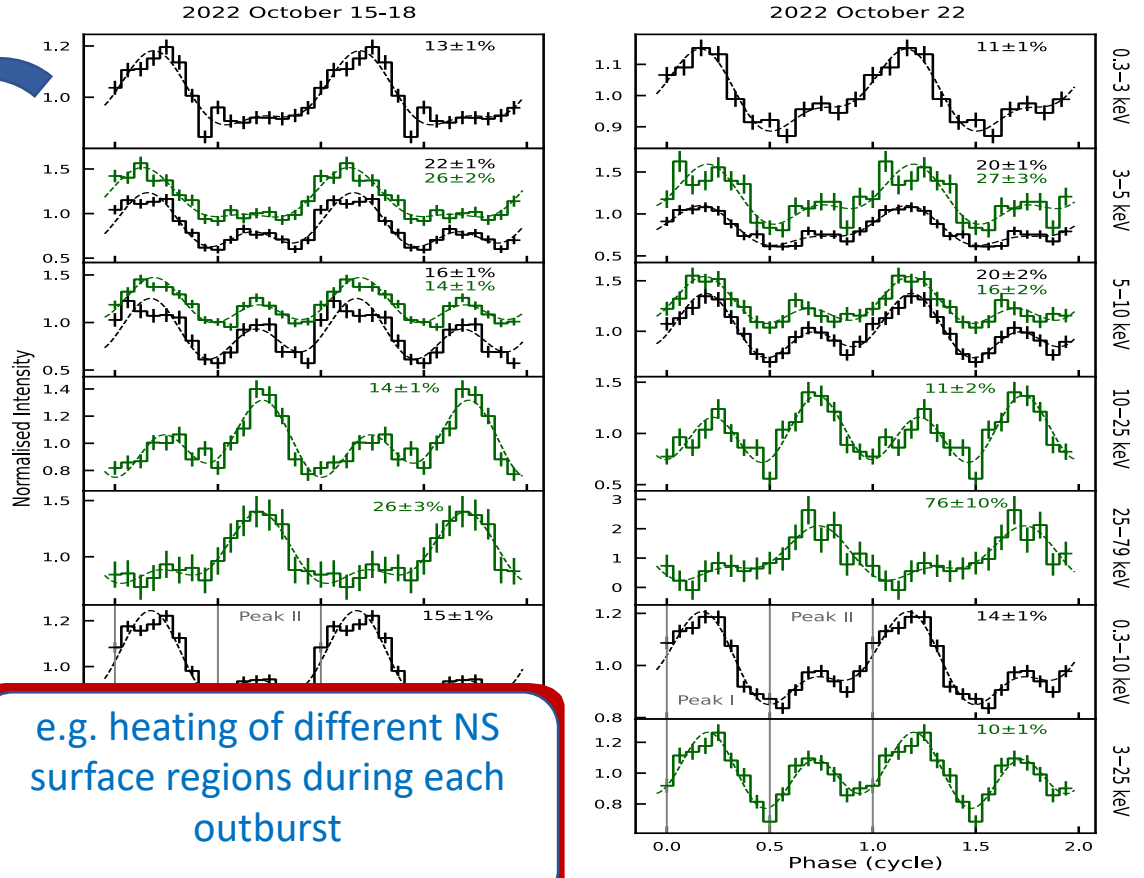

e.g. heating of different NS surface regions during each outburst

Israel et al. 2016

3.2. **Energy-resolved pulse profile**

- Cons + 2 sinusoidal function

(fundamental 1st harmonic components)

- Morphology evolution
- No specific trend in the PF

epoch1 (14-26) epoch2 (11-76)

$E_{25\text{-}79}$ (26 -76)

- Phase-resolved spectroscopy:

A phase shift: $soft_{(0.3-10)}$ /$hard_{(10-25)}$ (~$0.13_{P1Ep1,11}$ & $0.19_{PIIEp1,}0.22_{PIIEp2}$)

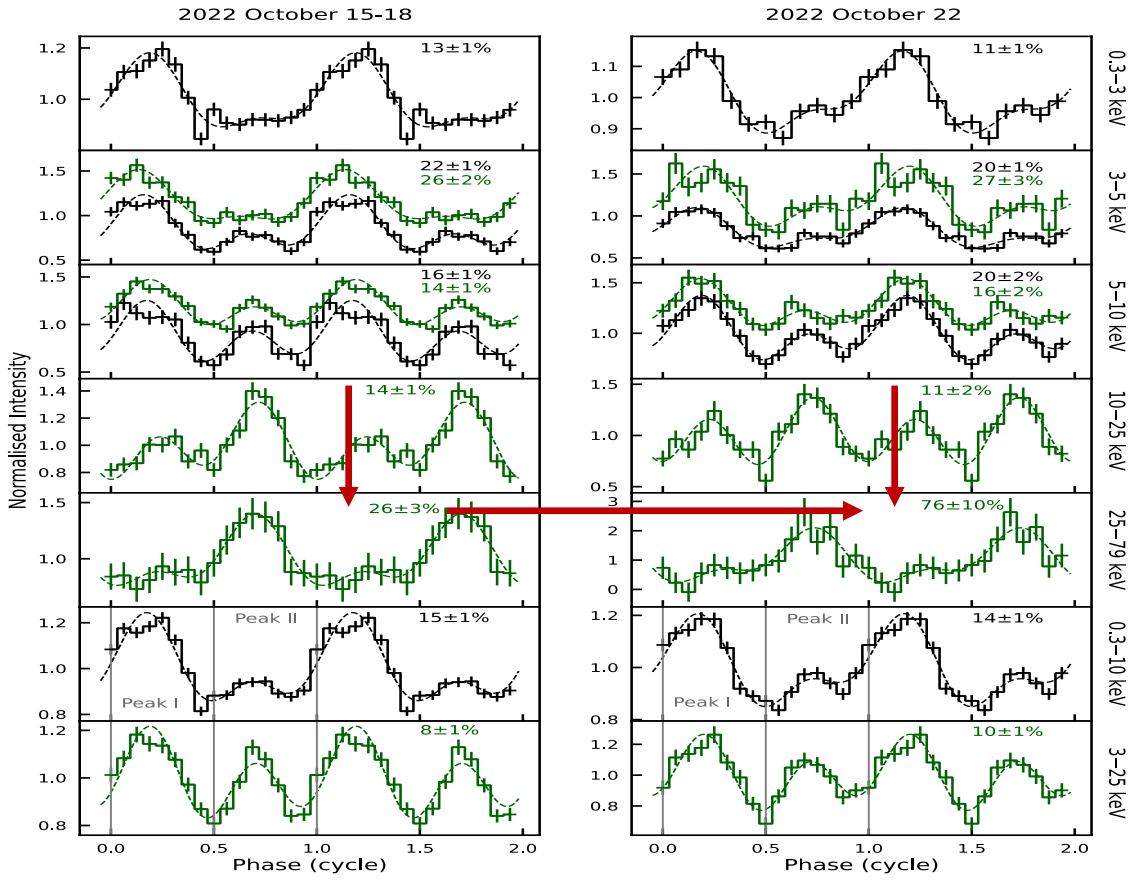

3.2. **Energy-resolved pulse profile**

- Cons + 2 sinusoidal function

(fundamental 1st harmonic components)

- Morphology evolution
- No specific trend in the PF

epoch1 (14-26) epoch2 (11-76)

E_{25-79} (26 -76)

- Phase-resolved spectroscopy:

A phase shift: $soft_{(0.3-10)}$ /$hard_{(10-25)}$ (~$0.13_{P1Ep1,11}$ & 0.19_{PIIEp1},0.22_{PIIEp2})

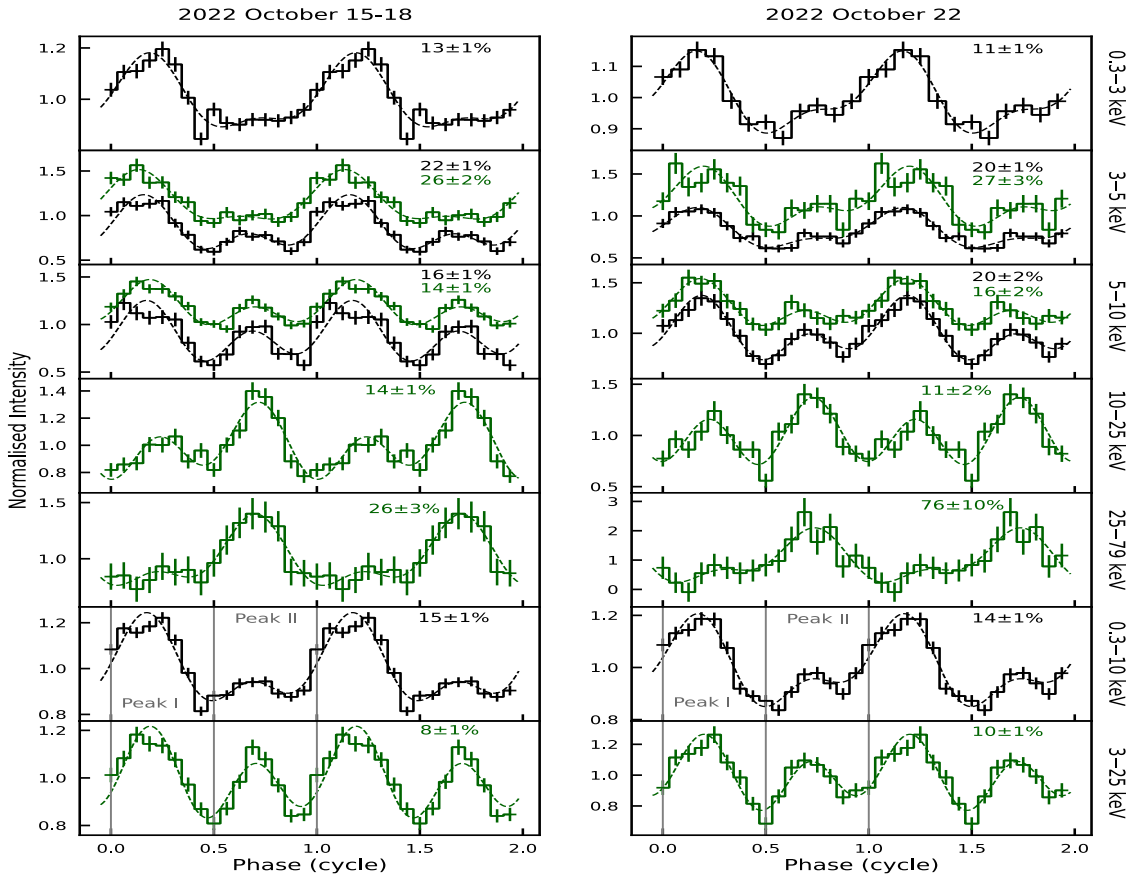

3.2. **Energy-resolved pulse profile**

- Cons + 2 sinusoidal function

(fundamental 1st harmonic component

- Morphology evolution
- No specific trend in the PF

epoch1 (14-26) epoch2 (11-76)

E_{25-79} (26 -76)

- Phase-resolved spectroscopy:

A phase shift: $soft_{(0.3-10)}$ /$hard_{(10-25}$ (~$0.13_{P1Ep1,11}$ & $0.19_{PIIEp1,}0.22_{PIIEp2}$)

e.g. non-thermal X-ray: resonant inverse Compton scattering of photons emitted from the star surface by charged particles

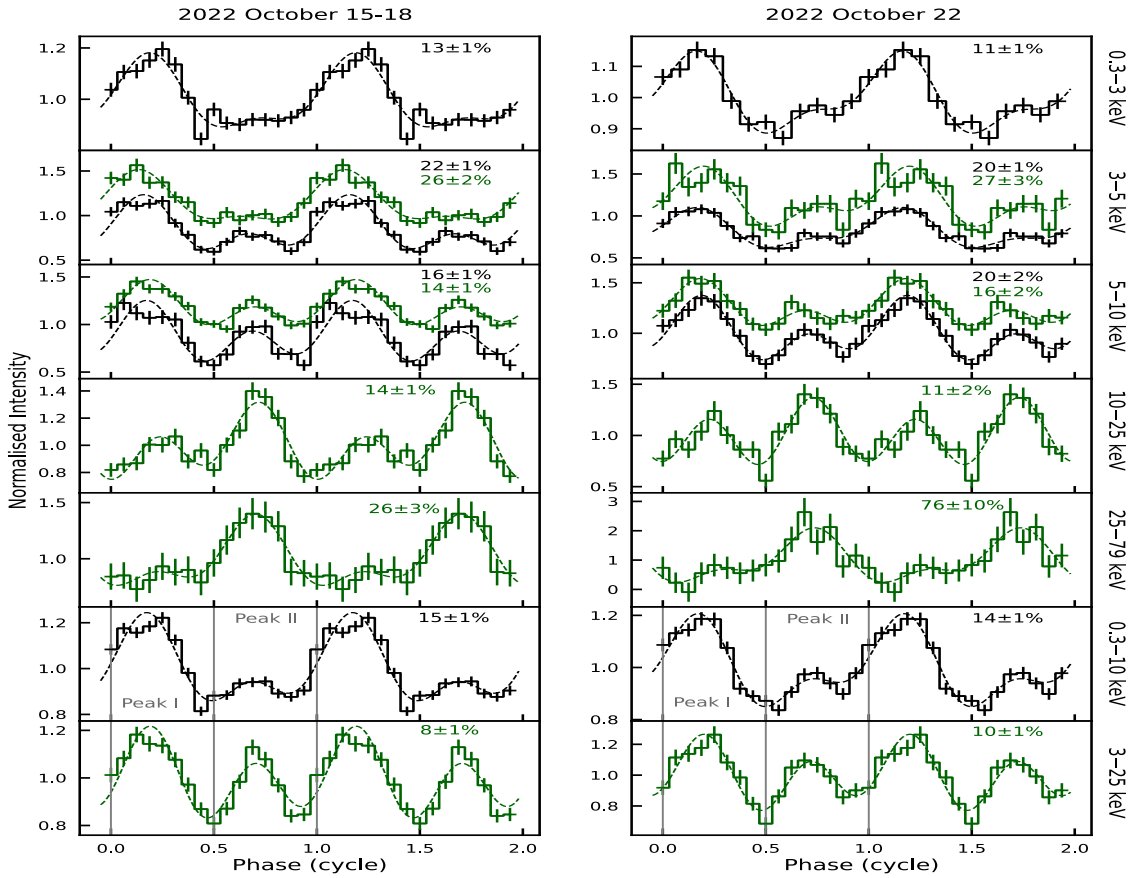

3.3. **Persistent spectra**

- con*tbabs*(bb+pl)
- $N_H \sim 2.57\ (0.05) \times 10^{22}\ cm^{-2}$
- $kT_{BB} \sim 0.4$ keV (no variation)
- $\Gamma \sim 1.51\ (0.02)$ & $1.41\ (0.02)$
- $\chi^2_{red} = 1.08$ (567 d.o.f)

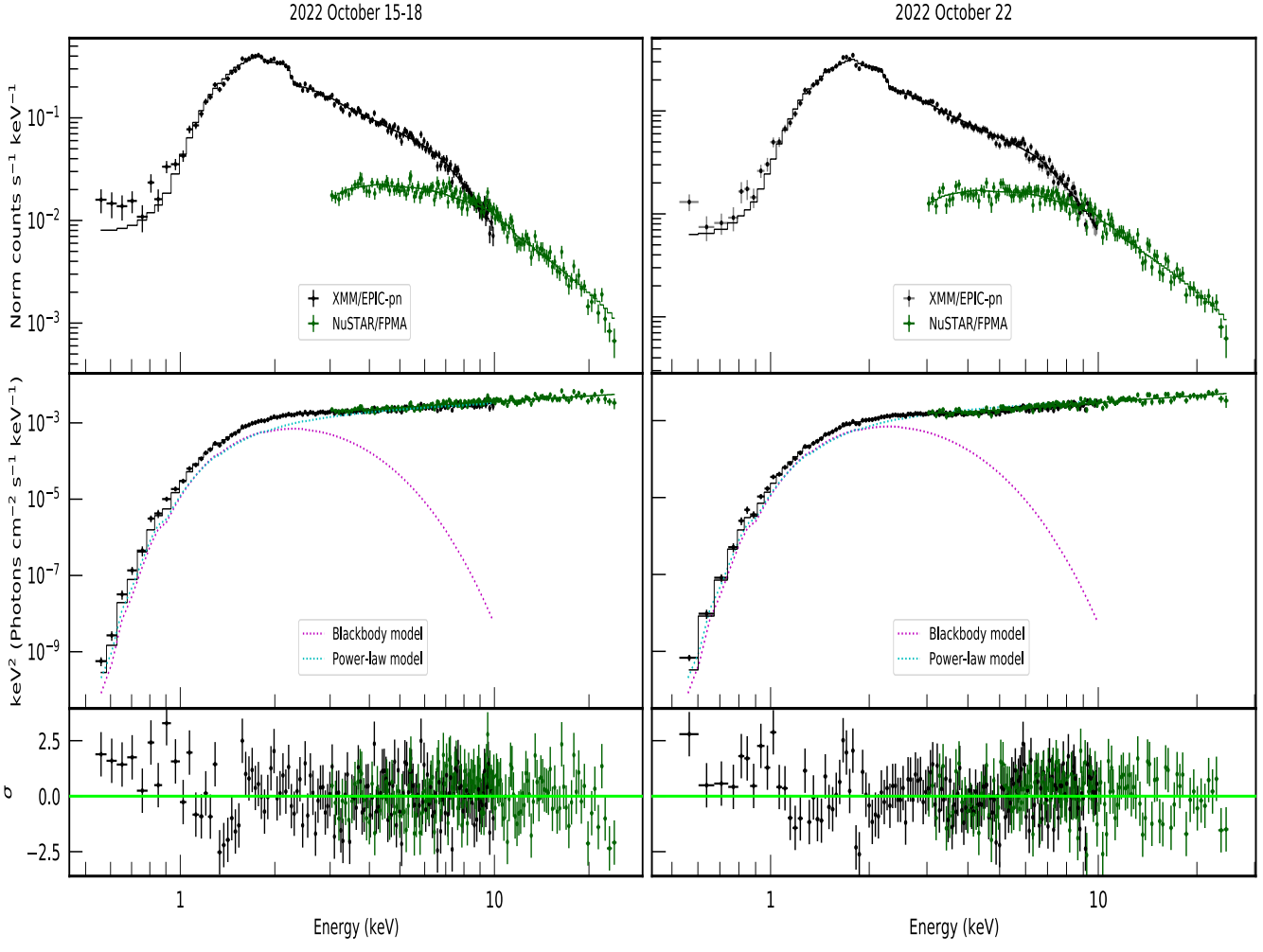

3.4. **Bursts search**

Total of 36 bursts

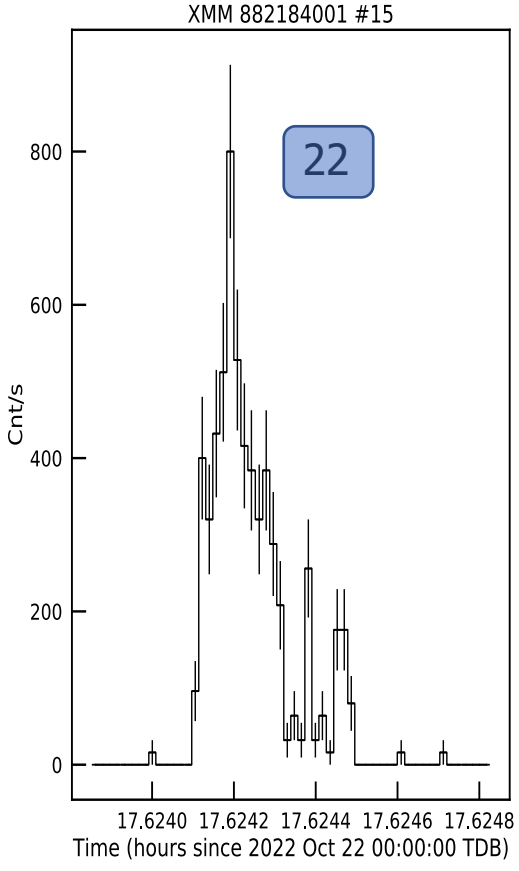

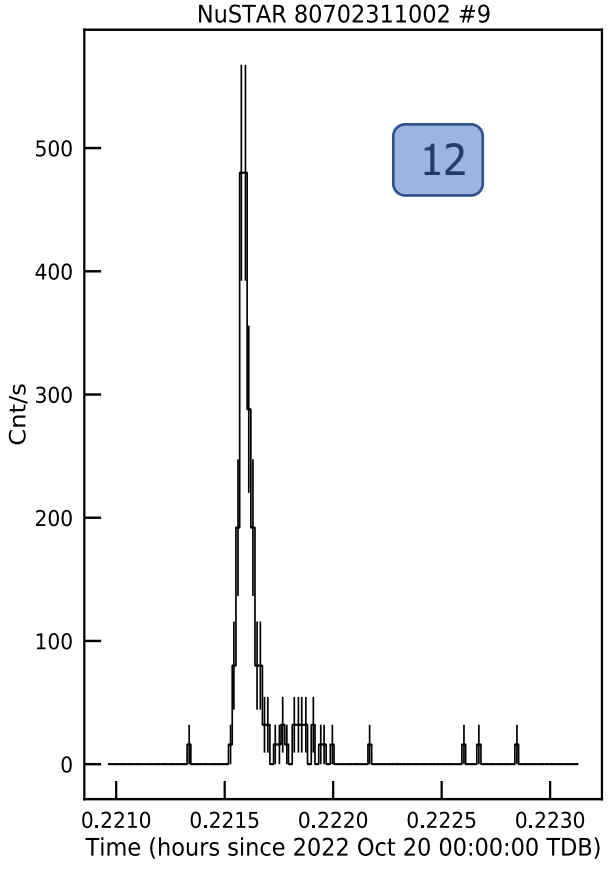

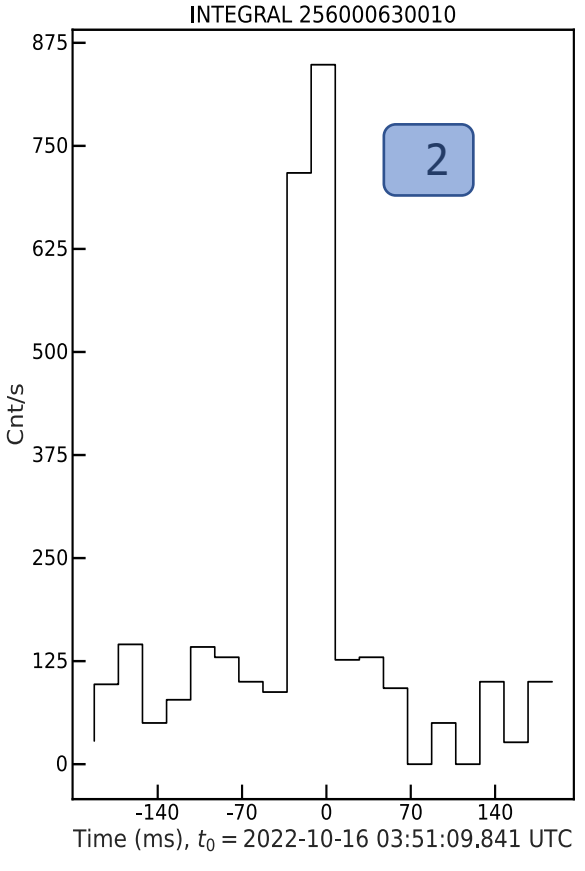

4. Conclusion

- **High Activity:** SGR J1935+2154 has been highly active since its discovery
- **FRB Link:** First link between magnetars and Fast Radio Bursts (FRBs)
- **Spin Period:** Spin period derivative is 3.8 times larger than in 2014
- **Emission Spectrum**: Persistent emission spectrum shows slight power-law variations with no significant change in blackbody temperature (kT_{BB})
- **Burst search:** 36 bursts

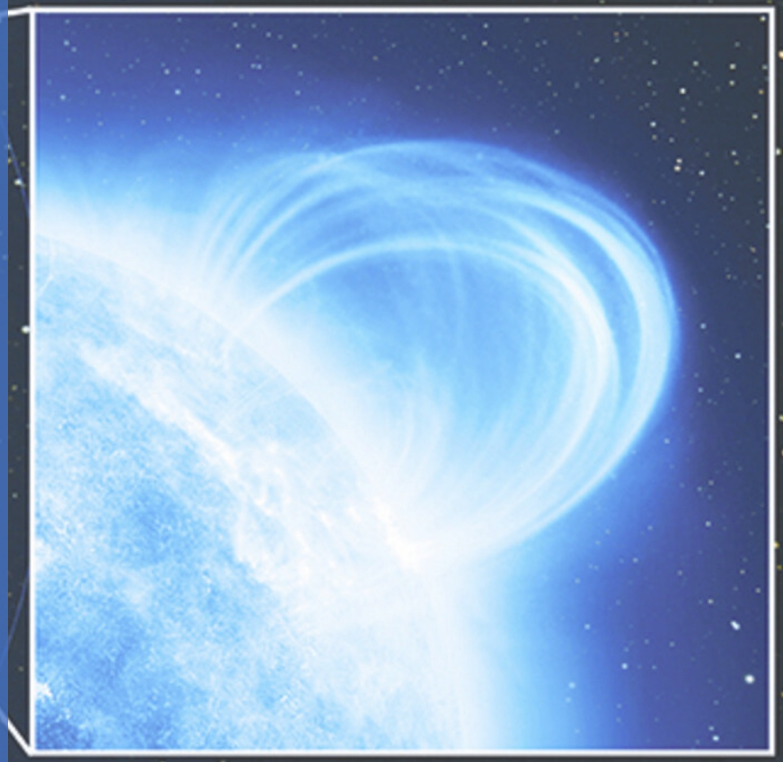

ESA/ATG Medialab

Thank you!

I.* Phase distribution of the bursts

- Rotation phase and burst epoch
- Burst cumulative distribution in phase consistent with the uniform distribution
- In agreement with Younes et al. 2020

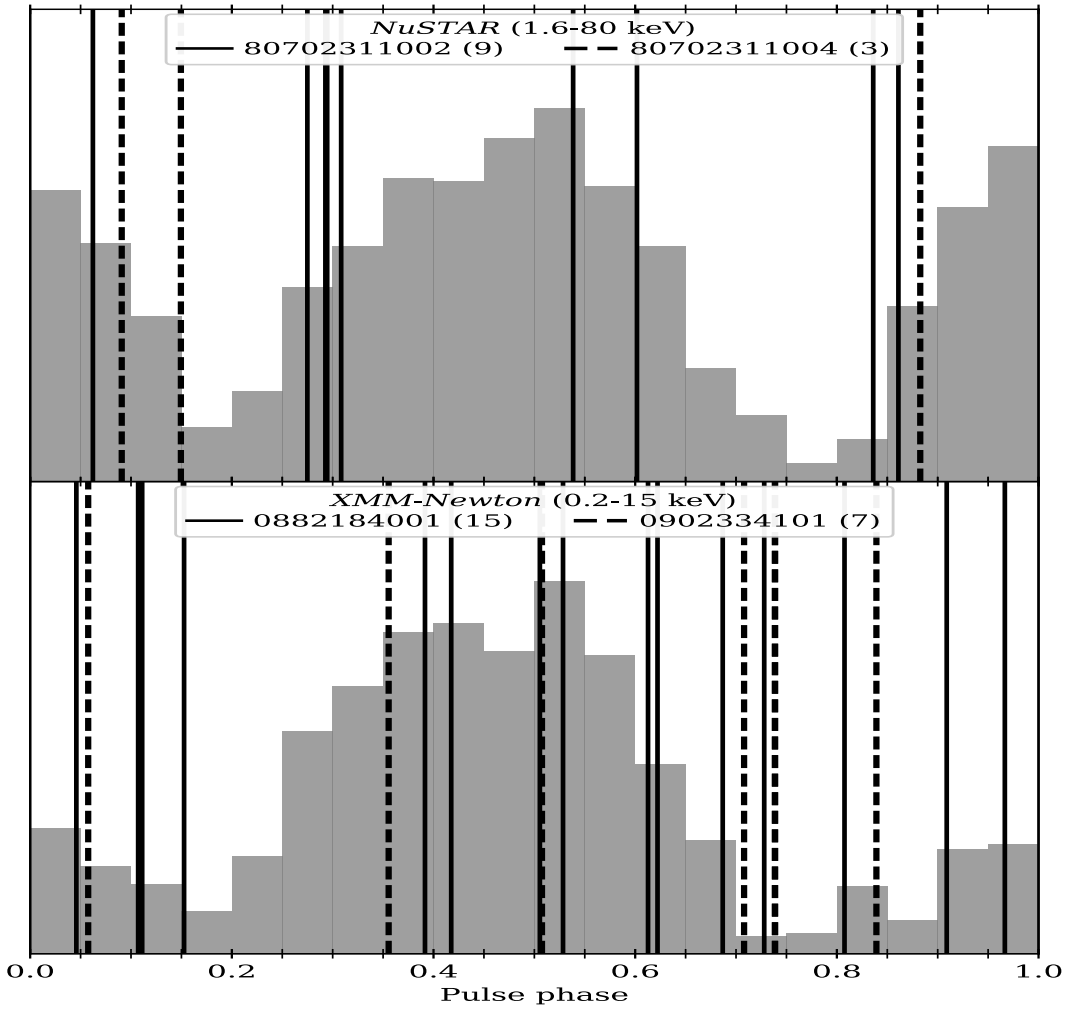

2.* Search for FRB-like bursts/Pulse emission

- October 15 and 19, 2022 for a total of 92.5 hr
- No FRB-like burst detection
- 900s scans folded in X-ray timing to create a single file (psradd) and check by psrplot
- No evidence for pulse radio emission

Table 3. Observational setup of the radio telescopes.

Station[a]	Band	Frequency Range [MHz]	Bandwidth[b] [MHz]	Bandwidth per subband [MHz]	SEFD[c] [Jy]	Completeness[d] [Jy ms]	Time observed [hrs]
Wb	P	300–364	50	8	2100	46	11.4
Wb	L	1207–1335	100	16	420	7	45.5
Tr	L	1350–1478	100	16	250	4	22.0
O8	L_{O8-1}	1360–1488	100	16	310	5	6.3
O8	L_{O8-2}	1594.49–1722.49	100	16	310	5	7.4
Total telescope time/total time on source [hrs][e]							92.5/60.4

[a] Wb: Westerbork RT1 25-m, O8: Onsala 25-m, Tr: Toruń 32-m

[b] Effective bandwidth accounting for RFI and band edges.

[c] From the EVN status page.

[d] Using Equation 1, assuming a 7σ detection threshold and a pulse width of 1 ms.

[e] Total time on source accounts for overlap between the participating stations.

Table 2. Results of the phase-resolved spectral analysis presented in Section 3.3.

2022 Oct 15–18						
	Phase	$kT_{\rm BB}$ (keV)	$R_{\rm BB}$ (km)	Γ	Flux[a] Unabs BB (10^{-12} erg cm^{-2} s^{-1})	Flux[a] Unabs PL (10^{-12} erg cm^{-2} s^{-1})
Peak I	0.0–0.5	0.42±0.02	1.3±0.1	1.58±0.04	1.38±0.02	7.36±0.01
Peak II	0.5–1.0	0.44±0.01	1.26±0.08	1.36±0.04	1.61±0.02	7.19±0.01
2022 Oct 22						
	Phase	$kT_{\rm BB}$ (keV)	$R_{\rm BB}$ (km)	Γ	Flux[a] Unabs BB (10^{-12} erg cm^{-2} s^{-1})	Flux[a] Unabs PL (10^{-12} erg cm^{-2} s^{-1})
Peak I	0.0–0.5	0.41±0.01	1.86±0.09	1.30±0.04	2.52±0.01	12.79±0.01
Peak II	0.5–1.0	0.41±0.01	1.83±0.09	1.43±0.04	2.38±0.01	10.05±0.01

[a] The fluxes are estimated in the 0.5–25 keV energy range.

3.2.* Phase-resolved spectroscopy

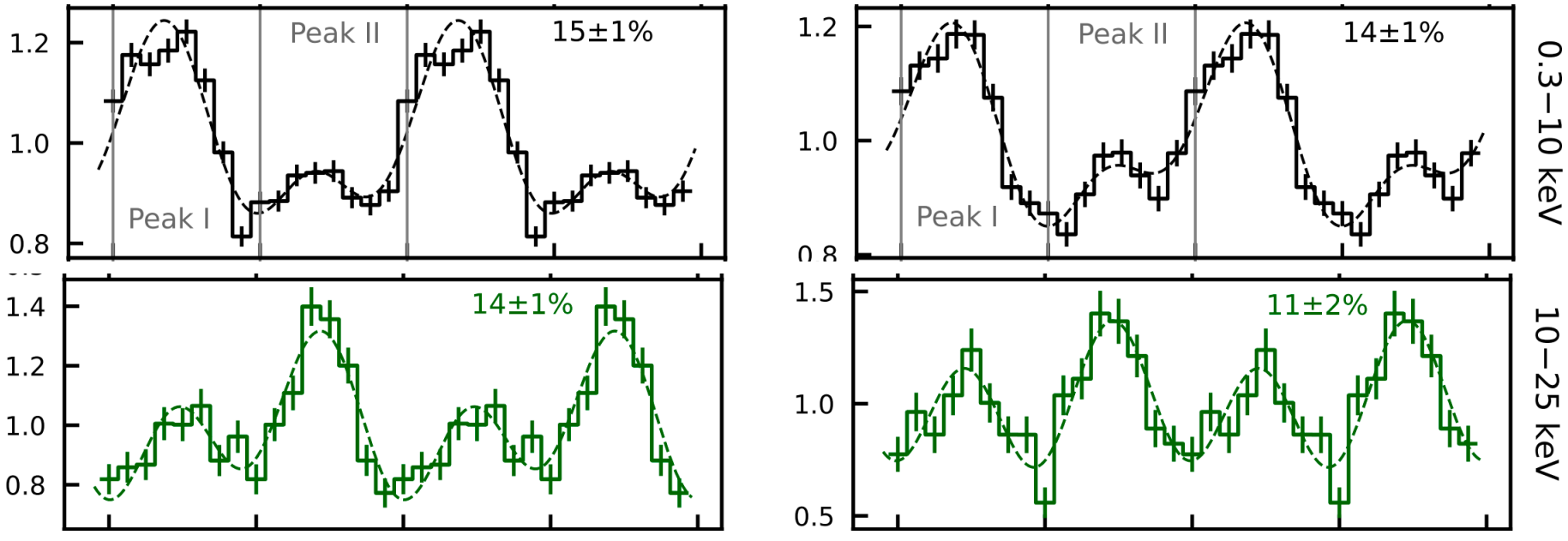

Table A1. Log of X-ray bursts detected in all datasets and results of the spectral analysis for the brightest events. The $N_{\rm H}$ has been fixed to the average value in the spectral fits.

Instrument/Obs.ID[a]	Burst epoch	Fluence	Duration	$kT_{\rm BB}$	$R_{\rm BB}$	$F_{\rm X,unabs}$[b]	χ^2/ W-stat (dof)
	YYYY-MM-DD hh:mm:ss (TDB)	(counts)	(ms)	(keV)	(km)	($\times10^{-9}$ erg cm^{-2} s^{-1})	
XMM/0902334101 #1†	2022-10-15 20:26:14.457	17	31.25				
#2†	2022-10-16 00:41:42.870	11	62.5				
#3⋆	03:53:09.083	55	109.375	1.5±0.2	$3.0^{+0.8}_{-0.6}$	0.9±0.1	χ^2=15.86 (14)
#4	10:35:28.285	31	62.5	$1.7^{+0.7}_{-0.4}$	$7.6^{+5.2}_{-2.4}$	10±3	W-stat=21.55 (11)
#5	10:45:11.000	10	62.5				
#6	10:45:14.351	61	109.375	$2.2^{+0.8}_{-0.5}$	$4.6^{+2.1}_{-1.2}$	9±2	χ^2=5.14 (6)
#7	12:05:02.934	29	62.5	$1.4^{+0.4}_{-0.2}$	$7.7^{+3.7}_{-2.0}$	5±1	W-stat=13.54 (16)
NuSTAR/80702311002 #1	2022-10-19 06:29:29.769	25	46.875				
#2	07:56:58.869	13	125				
#3	08:21:05.061	8	62.5				
#4	09:48:56.934	21	46.875				
#5†	11:33:02.606	20	46.875				
#6†	13:21:31.841	30	62.5				
#7†	17:24:38.512	12	31.25				
#8†	17:46:13.429	15	125				
#9	2022-10-20 00:13:17.634	80	171.875	$3.1^{+0.6}_{-0.4}$	$1.0^{+0.8}_{-0.6}$	1.2±0.2	W-stat=10.87 (17)
XMM/0882184001 #1	2022-10-22 03:59:47.011	16	62.5				
#2	04:27:31.542	9	31.25				
#3	04:46:13.754	110	218.75	$2.2^{+0.4}_{-0.3}$	$3.9^{+1.0}_{-0.7}$	5.9±0.8	χ^2=4.15 (6)
#4	04:53:17.448	20	62.5				
#5	05:01:16.104	14	62.5				
#6	06:12:48.464	20	125				
#7	06:18:35.417	28	93.75	$2.6^{+1.8}_{-0.7}$	$3.2^{+2.3}_{-1.1}$	7±2	W-stat=14.42 (13)
#8	09:29:20.325	27	93.75	$1.9^{+0.7}_{-0.4}$	$4.9^{+2.9}_{-1.4}$	6±2	W-stat=11.01 (14)
#9	10:01:26.472	132	187.5	$2.3^{+0.6}_{-0.4}$	$4.0^{+1.4}_{-0.9}$	7±1	χ^2=7.33 (6)
#10	14:18.57.919	27	125	$1.4^{+0.4}_{-0.3}$	$3.1^{+1.8}_{-0.8}$	0.8±0.2	χ^2=2.74 (4)
#11	15:41:35.417	12	62.5				
#12	16:25:01.920	30	156.25	$2.4^{+1.2}_{-0.6}$	$2.9^{+1.7}_{-0.9}$	4±1	W-stat=13.08 (18)
#13	16:31:33.816	123	203.125	$1.9^{+0.3}_{-0.2}$	$4.8^{+1.3}_{-0.9}$	5.3±0.7	χ^2=14.13 (8)
#14	16:42:44.030	28	125	$0.8^{+0.2}_{-0.1}$	$12.9^{+8.0}_{-3.7}$	1.5±0.4	W-stat=4.91 (8)
#15	17:37:26.814	290	531.25	2.1±0.2	$3.4^{+0.5}_{-0.4}$	4.0±0.3	χ^2=21.87 (24)
NuSTAR/80702311004 #1	2022-10-22 22:57:23.582	23	62.5				
#2	2022-10-23 21:58:05.838	10	62.5				
#3	22:50:23.135	27	62.5				

[a] The notation #N corresponds to the burst number in a given observation.

[b] The flux was estimated in the 0.5–10 keV range for *XMM–Newton* and *NuSTAR*.

† These bursts were covered by radio observations (for details, see Table A2).

⋆ Burst detected also with *INTEGRAL*.

2.1. SGR J1935+2154: Outbursts history

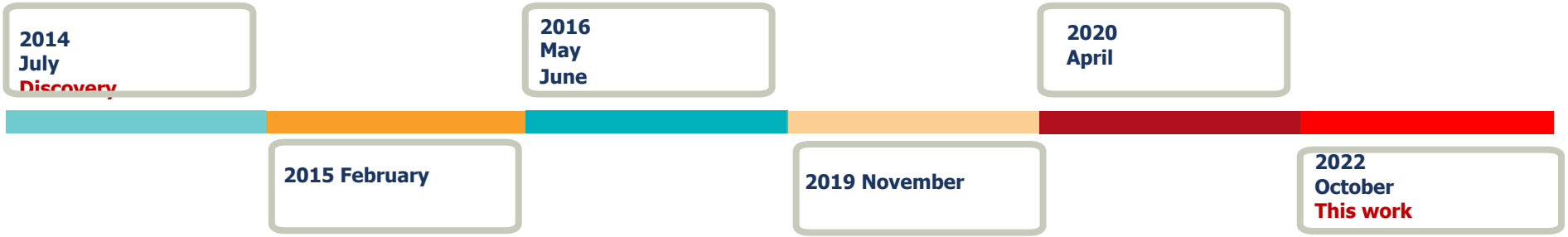

Israel et al. 2016; Younes et al. 2017,2020; Borghese et al. 2020, 2022; CHIME/FRB Collaboration et al. 2020, 2022; Ibrahim et al. 2022